

# Range Sections as Rock Models for Intensity Rock Scene Segmentation

*\*S. Mkwelo , \*\*G. De Jager and \*\*F. Nicolls*

\*Defence, Peace, Safety and Security,  
Council for Scientific and Industrial Research (CSIR), Lynnwood, Pretoria, South Africa  
\*\*Department of Electrical Engineering, University of Cape Town, Rondebosch, 7700  
fax: +27 841 2455  
smkwelo@csir.co.za

## Abstract

This paper presents another approach to segmenting a scene of rocks on a conveyor belt for the purposes of measuring rock size. Rock size estimation instruments are used to monitor, optimize and control milling and crushing in the mining industry. We propose a joint analysis of range and intensity images of rocks where sections extracted from range images are used to guide a Model-driven intensity image segmentation process. The models contain rock shape and edge probability information which can be used to extract intensity edges of relevance in terms of orientation and position. Conventional polynomial fitting is used to extract the underlying rock shape as a final segmentation. Preliminary results on a small laboratory data set using qualitative and quantitative measures of performance are promising.

## 1. Introduction

A rock-sizing instrument designed to operate in the harsh mining environment has benefits of monitoring, optimization and control of blasting and comminution. Image processing in particular, has been widely accepted as the analysis method of choice for the estimation of rock-size because of: the non-intrusive nature of the measurement process; the capability of measuring continuously and in real time; the repeatability of measurements given the same scene and lighting conditions; and the absence of moving mechanical parts which implies little or no maintenance.

Intensity image analysis, in particular, has been a research area of focus for many of the recent academic [2, 3, 4] and operational [1, 5, 6] systems, mainly because of financial viability coupled with the sensitivity of the imaging sensor to shadows which are formed around the individual particles. These shadows are detected and completed as rock outlines during rock scene segmentation. However, limitations of intensity sensors are well documented [7, 3]: the loss of a dimension due to the projective nature of the sensor; and the loss of small particles due to the limitation in the sensor's resolution, etc. These limita-

tions introduce errors into the measurement process which are further increased by errors that can be attributed to the environment under imaging: poor lighting; color density and texture variations.

Lighting conditions have been controlled through the elimination of natural lighting and proper design of synthetic lighting [3]. We present a methodology that avoids problems associated with texture and color density variations during rock edge extraction. The methodology uses range sections as models or a priori knowledge for model-based intensity edge detection. Experience and previous work [3] has shown that the human visual system (HVS) is more than capable of rock-scene segmentation and therefore serves as an inspiration to the adopted methodology. The HVS is known to use a priori knowledge or templates as part of object identification and recognition. In this work, rock sections are extracted from a range image as a pre-attentive process that forms models in memory. The information of interest from a model in the form of boundary shape and edge probability is used to guide intensity image segmentation. In order to obtain smooth and continuous shapes of rock boundaries, a statistical analysis of the detected edge pattern is performed. The statistical analysis involves outlier removal and polynomial curve fitting.

The rest of the paper is organized as follows: the extraction of range sections from a range image is described in section 2; template-based edge detection is presented in sections 3; Results of the work are presented in section 4; and conclusions are drawn in section 5.

## 2. Extraction of Range Sections

Segmentation of range data is an important part of range image perception and understanding. The general problem of range image segmentation is that of partitioning the range image into disjoint surfaces representing individual objects or a single object. The problem has seen many solutions such as the HK map iterative region growing[10], the effective jump-diffusion method[11], scan-line group-

ing [14], methods using mathematical morphology operators [12, 13] and others. In this work, the objective is to extract rock sections from a range image as they contain shape and edge probability information.

In [8, 9, 14], intensity and range data are fused in various ways to improve scene segmentation for various purposes. In this work, range segmentations are used to improve intensity image segmentation, see section 3. We extract range sections through a rock model extraction process, which is based on morphological operators as shown in figure 1. Specifically, gray-scale reconstruction, watershed and distance transforms are used, as shown in figure 1. In essence, the gray-scale reconstruction extracts the smallest sections as markers which are used for recovering optimum sections through a watershed process.

The first watershed is used to estimate a range threshold that separates foreground and background sections based on a discrepancy between trough and surface range values. The second watershed combined with the distance transform spatially splits connected sections that result from the previous process. Due to the nature of the distance transform, connected sections will have cone shaped structures whose peaks are centered at the centroids of the sections with local minima or saddle points between these peaks. This allows for a watershed transform to create boundaries at the saddle points and hence splitting connected sections.

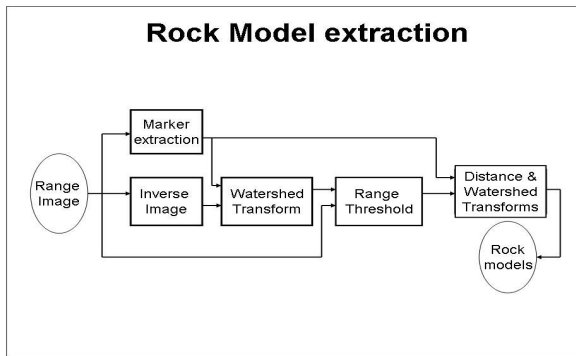


Figure 1: A block diagram representation of rock model extraction.

### 3. Model-driven edge detection

Perception and understanding of intensity data often requires image segmentation. The segmentation of intensity rock-scenes can be difficult without a priori knowledge about rocks because of noise, texture and color density variations on rock surfaces. Crida[3] used elliptical models of rocks as a priori knowledge for focused intensity edge detection. He used elliptical probability masks and edge orientations to limit the search for edge pixels. In

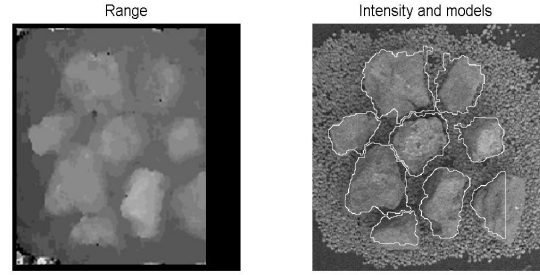


Figure 2: Intensity, range and rock sections

this work, a similar approach is taken, except rock sections from a range image are used to produce probability masks and edge orientations for rock template-based edge detection. The edge detection is local by nature and therefore focuses attention to a predefined region-of-interest.

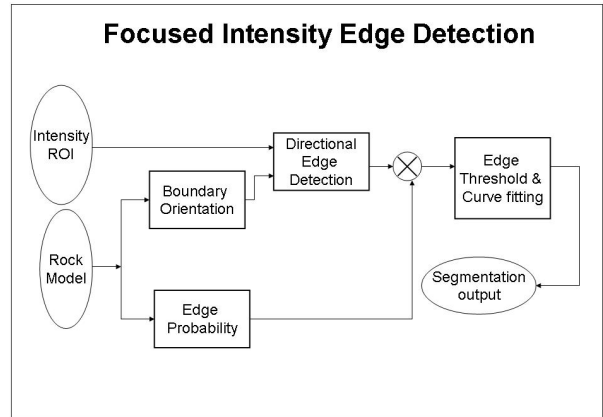


Figure 3: A block diagram representation of focused intensity edge detection.

Once a rock is identified and sectioned in a range image, the position and size of the sectional area is used to define a window around the corresponding intensity rock. As shown in figure 3, the boundary orientation of the section is used to perform directed edge detection, where edge templates are effectively aligned with the segments of the boundary. The edge probability, defined as the marginal band around the boundary that is most likely to contain actual intensity edges, is used to remove spurious edge responses through a masking operation. The result is optimized through a search for maximum edge responses along each radial line, outlier removal and curve fitting to obtain a continuous rock boundary.

#### 3.1. Edge detection, masking and optimization

The intensity rock is subjected to a non-linear edge detection method that computes edge-responses based on a [3-

by-3] kernel matrix whose elements depend on the pixel position and orientation of the boundary model at that point. The practical implementation involves predefining a set of possible kernels for a number of arc intervals of a circle. Each arc interval is assigned a specific kernel matrix.

The probability mask is used to spatially eliminate spurious edge responses. Its' creation involves a dilation of the sections boundary by predefined amount, distance transformation and normalization. This process assigns high probabilities to pixels on the central path of the marginal band. The masking is achieved by multiplying the edge response with a probability mask to produce a masked response with less spurious pixels. The masked response is then optimized by searching for pixels with maximum edge responses. Figure 4 shows input intensity, edge response, probability mask, masked response and optimized response sub-images.

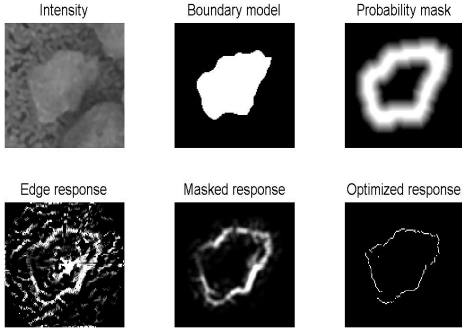


Figure 4: Image data: intensity, boundary model, probability mask, edge response, masked response and optimized response

### 3.2. Rock shape extraction

It is desirable to have a smooth and continuous curve to model the set of detected rock pixels. In this work, the detected pixels are transformed from an image to an angular-series representation. The independent variable becomes angle in radians and the dependent variable is the radial distance from the center of the section. The angles range from zero to  $2\pi$  radians and the distance signal wraps around at the zero and  $2\pi$  radians interface. A circle of radius  $r$  in an image becomes a DC signal of  $r$  volts in the angular-series representation. An ellipse becomes an approximately sinusoidal signal with a DC offset equal to the average of the principal components and amplitude equal to the difference in principal components, as shown in figure 5.

In general, however, ore can consist of particles with sharp and pointed edges producing irregular and complex angular-series. We use an  $N^{th}$  order least squares poly-

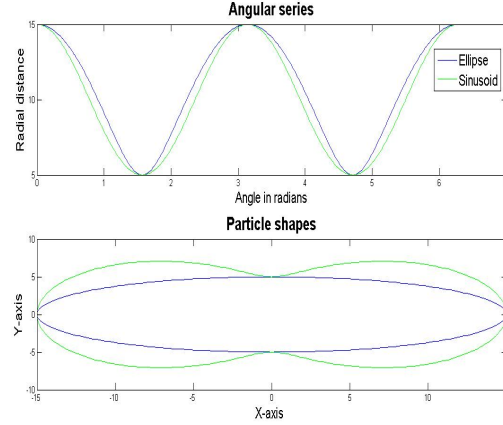


Figure 5: A sinusoidal signal as an approximation to an elliptical shape.

mial as a first approximation to the angular-series points and hence extract the underlying shape of the projected rock. The least squares formulation determines coefficients  $\mathbf{c} = [c_N, c_{N-1}, c_{N-2}, \dots, c_1]^T$  from the general vector equation  $\mathbf{y} = \mathbf{A}\mathbf{c}$  as being  $(\mathbf{A}^T\mathbf{A})^{-1}\mathbf{A}^T$ . This is known as the pseudo-inverse of matrix  $\mathbf{A}$ . A single row of the matrix  $\mathbf{A}$  has the form  $[x^N x^{N-1} x^{N-2} \dots 1]$ . Least squares is known to perform well provided that there is an effective pre-processing for removing outliers in the data. Because it is not possible to completely remove outliers, it maybe necessary to investigate other curve fitting methods such as Radial Basis functions and robust estimation methods which are known to be less sensitive to outliers.

## 4. Methodology

The system's performance is evaluated in terms of a visual measure of error from images coupled with numerical errors between automatically extracted rock-shapes and hand segmented sub-images. Numerical differences in enclosed areas between the segmentations of the system and the human visual system are computed by image subtraction of the system output from the hand segmented images. The overall error is divided into over-estimation and under-estimation errors. The percentage error is computed relative to the HVS segmentations. Table 1 shows the user input parameter set that is used during the experiments and figure 2 is the input data-set to be used by the focused intensity segmentation algorithm.

## 5. Results

This section presents results on a data-set of 8 sub-images. The results are divided into visual and numerical categories based on performances with settings of table 1. The visual data in the form of the input intensity image, extracted model, angular series and segmented rock are shown

Table 1: *The user-input parameter set*

Parameter	value
Polynomial orders	11 and 15
Probability mask width	60% of radial distance
2-tail outlier search regions	50% of range
Intensity Gaussian filter [ <i>size</i> , $\sigma$ ]	[9, 0.5]

in figures 6 to 13. Polynomial fitting results with polynomials of order 15 and 11 are shown. The results show, as predicted, that the order 11 polynomial imposes smoothness on the model, while the 15<sup>th</sup> order can model the intricate complexities of rock shapes. The 15<sup>th</sup> order polynomial is used for comparisons to hand segmented sub-images.

Table 2: *Segmentation error with respect to HVS segmentation results*

Image	under-estimation	over-estimation	overall
image 1	1.85%	4.09%	5.93%
image 2	9.95%	2.96%	12.9%
image 3	2.04%	6.55%	8.59%
image 4	24.81%	0.24%	25.5%
image 5	1.07%	3.17%	4.24%
image 6	18.83%	1.82%	20.65%
image 7	0.92%	4.92%	5.84%
image 8	5.14%	1.66%	6.80%

Table 2 shows the numerical results of a comparison to hand segmented sub-images in terms of over-estimation, under-estimation and overall errors. Results show that the worst performance is produced on image 4 of figure 9, with an overall pixel error 25.5% and an under-estimation component of 24.81%. This image appears not to have clear indications of rock edges of interest. The system performs best on image 5 of figure 10, with a minimum overall error of 4.24%. This image appears to have very good edge information about the rock of interest. Image 3 of figure 8 exposes the effect of the sensitivity to outliers of the least squares method. As a result the overall error of 8.59% has an over-estimation component of 6.55%. Even though, the overall average error of 11.31% is promising, it is not a reliable measure of the system’s performance as the number of images is not sufficient.

## 6. Conclusions

Based on the above findings and results, the following conclusions can be drawn.

- A methodology for rock-scene segmentation that combines intensity and range image analysis to reduce the effects of texture and color density variations is presented.

- Post-processing in the form of outlier rejection and angular-series analysis ensures that the underlying rock-shape is extracted with good boundary accuracy. However, the least squares estimator of the fitting is sensitive to outliers and therefore other estimators must be investigated.
- A quantitative performance metric and more data are required for a more convincing performance evaluation.

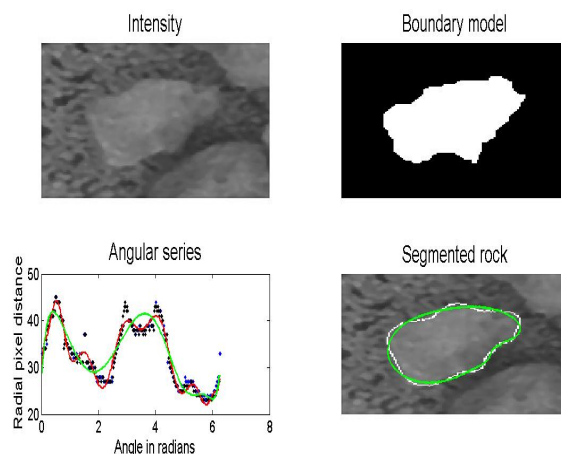


Figure 6: Rock image 1 results

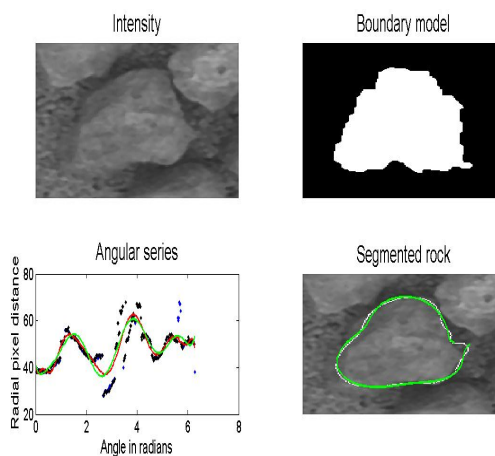


Figure 7: Rock image 2 results

## 7. Acknowledgements

The Author is grateful to the CSIR DPSS, Anglo-platinum, MPRU, UCT and NRF for financial support.

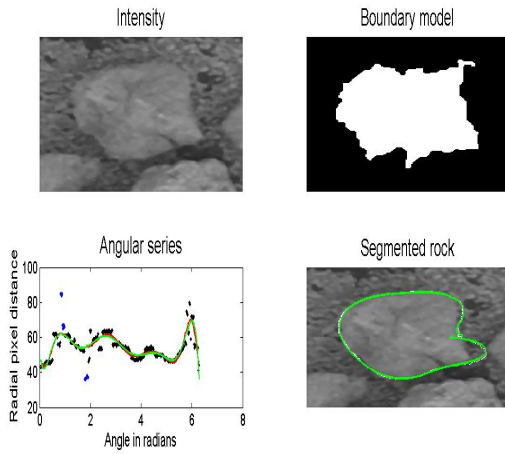


Figure 8: Rock image 3 results

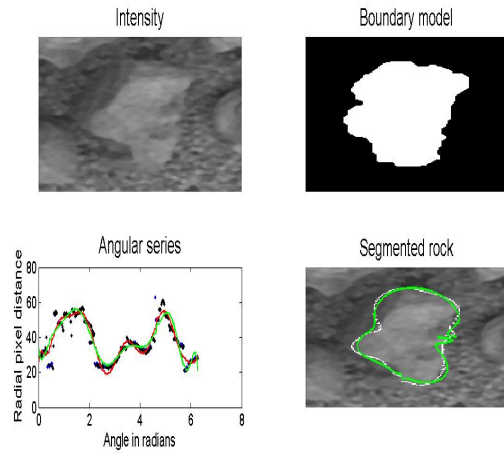


Figure 11: Rock image 6 results.

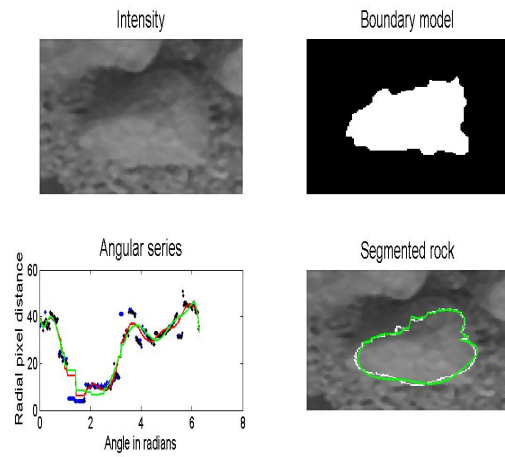


Figure 9: Rock image 4 results.

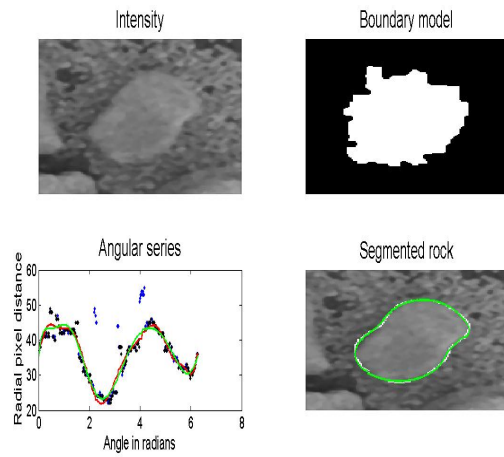


Figure 12: Rock image 7 results.

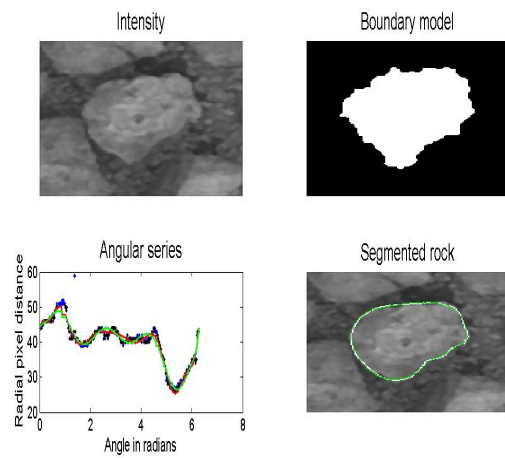


Figure 10: Rock image 5 results.

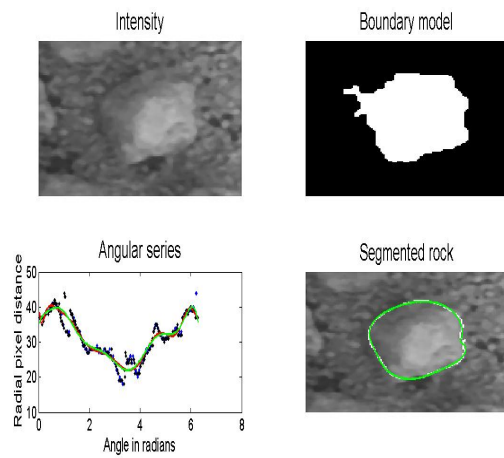


Figure 13: Rock image 8 results.

## 8. References

- [1] J. Sudhakar, G.R. Adhikari, R.N. Gupta, "Comparison of Fragmentation Measurements by Photographic and Image Analysis Techniques", *Rock Mechanics and Rock Engineering*, Springer-Verlag, pp. 159-168, 39(2), 2005.
- [2] Lange T.B, "Measurement of the size distribution of rocks on a conveyor belt using machine vision", PhD thesis at the University of Witwatersrand, 1990.
- [3] Crida R.C, "A machine vision approach to rock fragmentation", PhD thesis at the University of Cape Town, 1995.
- [4] S. Mkwelo, G. De Jager, F. Nicolls. "Watershed-based segmentation of rock scenes and proximity-based classification of watershed regions under uncontrolled lighting", *SAIEE Transactions*, research journal of SAIEE. VOL 96, NO. 1, 28-34, 2005.
- [5] Kemeny J., "The Split-Online Fragmentation Analysis System", [www.spliteng.com/split-online/fragmentation.asp](http://www.spliteng.com/split-online/fragmentation.asp), 12 February 2006.
- [6] Franklin J., "Granulometry Analysis Software", [www.wipware.com/wipfrag.php](http://www.wipware.com/wipfrag.php), 12 February 2006.
- [7] N.H. Maerz and W. Zhou. "Optical digital fragmentation measuring systems-inherent sources of error", *FRAGBLAST The international journal for blasting and fragmentation*, Volume 2, number 4, 415-431, 1998.
- [8] Neira J., Tardos J.D, Horn J, Schmidt G., "Fusing range and intensity images for mobile robot localization", *IEEE Transactions on robotics and automation*, vol. 15(1), February 1999.
- [9] Umeda K, Arai K., "Industrial vision system by fusing range and intensity image", *Proc. of IEEE Int. Conf. on Multisensor fusion and integration for Intelligent Systems*, 2-5 October 1994. classification: An experiment in human form detection", *International Conference on Image Processing*, Santa Barbara, October 26-29, 1997.
- [10] P.J. Besl, R.C. Jain. "Segmentation through variable order surface fitting" *IEEE Trans. on Pattern Analysis and Machine Intelligence*, PAMI-10, n. 2, pp. 167-192, 1988.
- [11] F. Han, Z. Tu, S. Zhu. "Range image segmentation by an effective jump diffusion method". *IEEE Transactions on pattern analysis and machine intelligence*, volume 26, number 9, September 2004.
- [12] L.A Gee, M.A. Abidi. "Segmentation of range images using morphological operations: Review and examples". *SPIE Conference on Intelligent Robots and Computer Vision XIV*, volume 2588, Philadelphia, PA, pp. 734-746, October 1995.
- [13] M.J Thurley. "Three dimensional data analysis for separation and sizing of rock piles in mining". PhD Thesis, Monash University, Department Electrical and Computer Systems Engineering, 2002.
- [14] Y. Zhang, Y. Sun, H. Sari-Sarraf, M. A. Aidi "Impact of Intensity Edge Map on Segmentation of noisy range images", *Proc. of Spie Conf. on Three Dimensional Capture and Applications III*, vol. 3958, pp. 260-269, San Jose, CA, 2000.